The International Journal of Advanced Manufacturing Technology (2022) 120:1203–1217
https://doi.org/10.1007/s00170-022-08877-y

ORIGINAL ARTICLE

Influence of the roll leveler setup parameters on the quality of high-strength steel leveling operation

Konrad Perzynski[1,2] · Kamil Pyzynski[2] · Sebastian Swierczynski[2] · Valeriy Pidvysots'kyy[3] · Janusz Klis[2] · Lukasz Madej[1,2]

Received: 5 May 2021 / Accepted: 2 February 2022 / Published online: 11 February 2022

Abstract
The computer-aided development of the leveling technology for high-strength steel flat sheet products is the primary goal of the research. The roll leveler setups are evaluated from the final product point of view with an acceptable flatness level and stress state at the same time. First, a reliable hardening model is developed based on experimental and numerical investigation. The combined isotropic-kinematic model is selected to capture material behavior under cyclic loading conditions. The inverse analysis approach is used for the high-quality model parameters identification stage. Then the roll leveling process for a wide range of machine setups is simulated using a finite element model. Examples of results in the form of final flatness and stress distributions are presented within the work. As an outcome, a set of process parameters is identified that provides a good quality product for both investigated criteria.

Keywords Cold leveling · Cyclic deformation · Numerical modeling

1 Introduction

Continually increasing quality requirements from the modern automotive, machine, or railway industries force manufacturers to deliver components with strict geometrical tolerances. For the production of such components, precise metal forming and subsequent machining, plasma, or laser cutting equipment are required. However, the main problem in this case, especially in the sheet-forming industry, is the springback effect [1] due to the residual stresses that are present in the formed components. Such a situation generates technical problems and can also damage the equipment, resulting in production lines' costly downtime. As a consequence, timely order fulfillment is jeopardized, while material and labor costs increase. Therefore, the input sheet material's quality after rolling for subsequent processing operations, e.g., bending, stamping, etc., is important [2]. In this case, the leveling operations based on roll levelers are often used to improve the quality of steel sheets before further processing [3]. The process is based on a series of cyclic deformations induced by a set of work rolls with specific diameter *D* and roll spacing *S* (Fig. 1).

The computer-aided technology design is an efficient tool to develop the leveling operation setup that can deliver not only flat sheets but also sheets with a low level of residual stresses. Models with various levels of complexity, including analytical [4, 5], semi-analytical [6], and numerical approaches [7] were developed for this task.

However, in the case of numerical modeling, material behavior under processing conditions always depends on the correctness of material properties' description. The accurate definition of the mechanical conditions is equally important. All the significant mechanisms responsible for material deformation have to be considered in the material model used during simulations.

Material models for the generally proportional deformation processes that are common in the cold metal-forming industry are based on simple closed-form [8] and differential [9] equations. They assume that the flow stress value increases due to the hardening phenomenon up to the plateau region with the increasing deformation. This plateau is a result of the interaction between hardening and recovery phenomena [10]. Therefore, these hardening models assume expansion of the yield surface without any change in its center position (Fig. 2a). However, when the investigated metal-forming process involves

✉ Lukasz Madej
lmadej@agh.edu.pl

1 AGH University of Science and Technology, Mickiewicza 30 av, 30-059 Krakow, Poland

2 ArcelorMittal Downstream Solutions Poland, Lowinskiego 15 st, 31-752 Krakow, Poland

3 Lukasiewicz Research Network - Institute for Ferrous Metallurgy, K. Miarki 12-14 st, 44-100 Gliwice, Poland

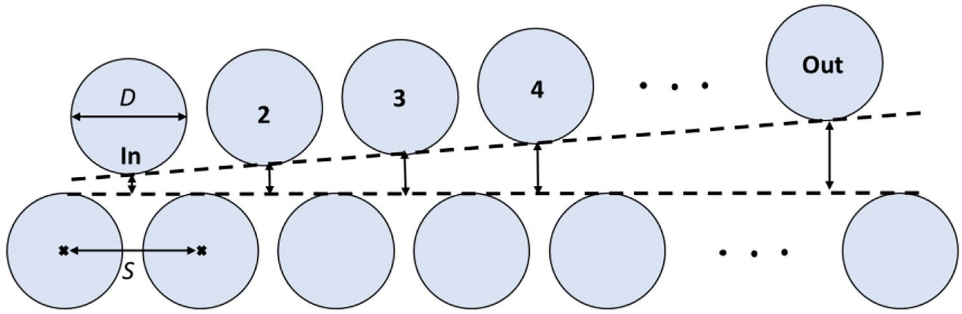

Fig. 1 Concept of the work rolls setup in the leveler

cyclic loading conditions, these conventional, isotropic hardening models fail to capture material behavior adequately. The reason for that is the Bauschinger effect [11], which reflects a transient decrease in the work hardening rate due to the occurrence of a significant change in the loading direction. In this case, when the processed material is subjected to loading under tension, the yield stress (σ_t) occurs at some specific level. When the loading direction changes and the sample is under compression, the yield stress (σ_c) is reduced due to the local rearrangement in the dislocation structures. The concept of the Bauschinger effect is schematically presented in Fig. 2b.

In the mentioned leveling operation on the roll leveler, cyclic loading is the primary loading mechanism leading to the steel plates' cold rectification. Therefore, the conventional hardening models affect the quality of the simulation results. As such, more advanced models taking into account the Bauschinger effect have to be considered.

In this regard, the most accurate approach is a combined model type, which couples the mentioned isotropic hardening model with the kinematic one. The latter can include the effects of cyclic changes in the loading direction as the center of the yield surface is no longer fixed and can move across the stress space (Fig. 2c). There are various combined type models with different complexity levels, see, e.g., [12–14]. The concept of the Lemaitre and Chaboche [14] was selected in the current research to identify the influence of the roll leveler setup parameters on the quality of high-strength steel after the leveling operation. With that, the guidelines for the roller leveling operation can be formulated to deliver good quality products.

2 Flow stress model development

As mentioned, the combined isotropic-kinematic hardening model was selected for the current study. In this approach, the isotropic part is expressed as

$$\sigma = \sigma_0 + \exp(a\varepsilon)^n \tag{1}$$

where σ_0 is the stress at the beginning of plastic deformation, ε the strain, n the coefficient of the sensitivity of flow stress to strain, and a the hardening coefficient.

The accompanying kinematic part has the following form:

$$\dot{\alpha} = C\frac{1}{\sigma}(\boldsymbol{\sigma} - \boldsymbol{\alpha})\dot{\varepsilon} - \gamma\boldsymbol{\alpha}\dot{\varepsilon} + \frac{1}{C}\boldsymbol{\alpha}\dot{C} \tag{2}$$

where α is the back stress tensor affects the yield surface center ($\sigma - \alpha$), σ the size of the yield surface, C, and γ the temperature-dependent parameters.

Developing a reliable flow stress model for further numerical simulations is always related to the model parameter identification procedure. In the current study, the inverse analysis concept [15] was applied. This approach is used to determine the flow stress model parameters directly based on the experimental load–displacement measurements. The procedure involves the experimental investigation of the cyclic plastometric test, developing the numerical model of the experimental setup, and applying the optimization method according to the diagram from Fig. 3. The advantages of this approach in identifying the combined hardening model parameters were proven in [16].

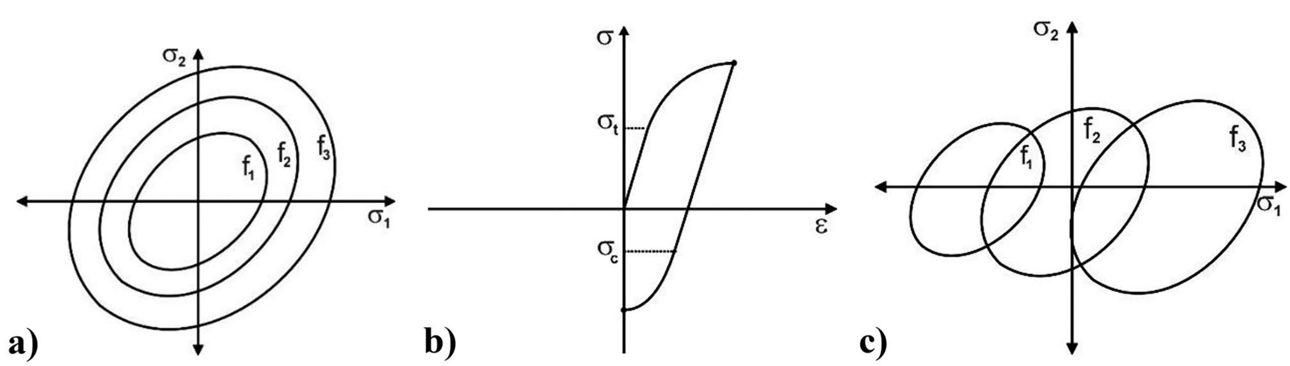

Fig. 2 The concept of the **a** isotropic hardening, **b** Bauschinger effect during reverse loading (tension/compression), and **c** kinematic hardening

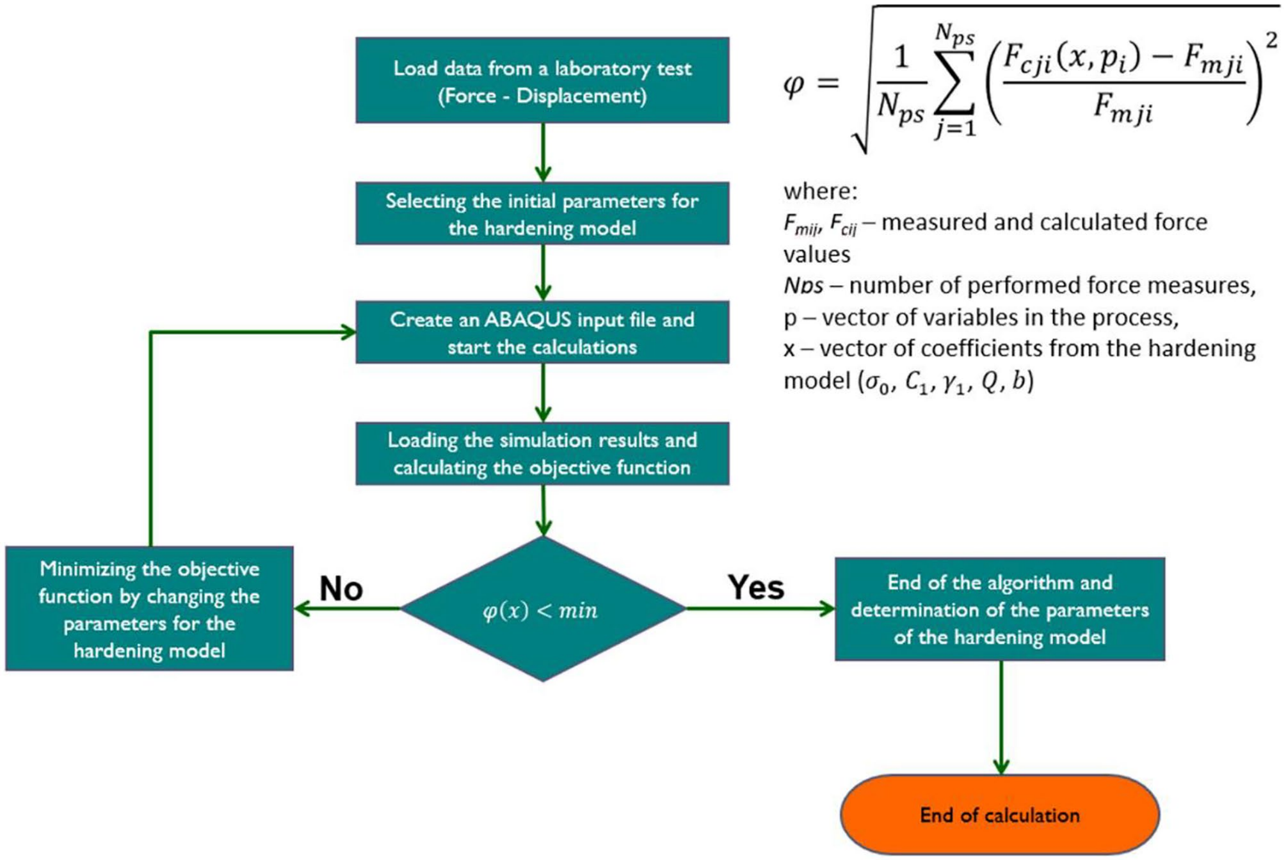

Fig. 3 Inverse analysis algorithm for the tension/compression experimental setup

The material under the investigation is industrial grade S700MC high-strength steel with the following chemical composition: C = 0.12, Si = 0.6, Mn = 2.1, Mo = 0.5, V = 0.2, Nb = 0.09, and Ti = 0.2. The mechanical properties that were determined during the uniaxial tensile test are gathered in Table 1. Samples for the investigation were cut out from industrial coil with thicknesses of 3, 5, and 10 mm and at 0, 45, and 90° in relation to the rolling direction to take into account the effect of anisotropy.

The obtained results did not show a major influence of sheet thickness on mechanical properties. Also, the anisotropy coefficient is typical for such a steel grade. Therefore, subsequent tests were realized only on one sheet thickness, and samples were cut out along the rolling direction. In this case, the cyclic tension/compression test was selected to replicate material behavior during the leveling operation due to its straightforward realization. Cylindrical specimens with 50-mm gauge length were used during the investigation, as seen in Fig. 4. For the accurate measurement of the elongation, an additional extensometer was applied. The cyclic experiments were carried out using the Gleeble 3800 thermomechanical simulator, as seen in Fig. 4b.

The experimentally measured load–displacement values were then used as an input for the inverse algorithm. The algorithm is based on the direct problem formulation, a finite element (FE) numerical model of the test. The numerical model of the tension/compression test was developed within the commercial Abaqus FE software and exactly replicated the Gleeble setup described above, as seen in Fig. 5.

Due to the sample's axisymmetric shape, the model order reduction technique [17] was used during the analysis. In this case, the model's dimensionality was reduced to 2D space after introducing the axial symmetry axis. This approach allows obtaining numerical results that are more accurate than in the 3D model by enabling the use of a significantly higher number of finite elements in the mesh. Additionally, to reduce the computational effort, which is the primary problem in the inverse analysis, the research area was limited only to the sample's gauge length, which is illustrated in Fig. 6.

A series of numerical calculations were performed based on the developed FE model during subsequent inverse procedure iterations. Examples of the distribution of equivalent stress and strain field at the sample's cross-section are shown in Fig. 7.

Table 1 Mechanical properties of the S700MC steel from 9 tests

R_{eH} ($R_{p0.2}$) [MPa]	636–826
R_m [MPa]	756–833
E [GPa]	149–234
A_{gt} [%]	9.3–11.7
A (A_{80mm}) [%]	17.5–41.5
$\bar{r}$	0.93–1.14

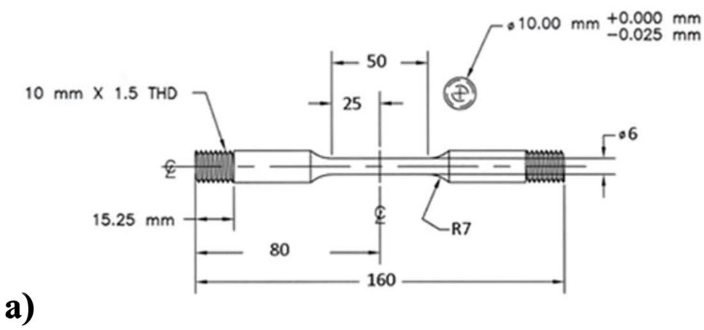

Fig. 4 **a** Dimensions of the tension/compression sample, **b** location of the sample within the Gleeble 3800 thermomechanical simulator

In each iteration of the inverse analysis algorithm, the FE model predicted the load values as a function of anvil displacement. These data and analogous experimental measurements were used to calculate the objective function value from Fig. 3. Minimizing the objective function with respect to combined hardening model parameters is the primary goal of the inverse investigation. The classical non-gradient Simplex optimization [15, 18] method was used during the model identification procedure.

The identified model parameters are presented in Table 2, while the corresponding agreement between the experimental and calculated loads during subsequent cyclic deformations is shown in Fig. 8.

Such a developed flow stress model considered the Bauschinger effect and was further used for the numerical simulation of leveling operations.

3 Leveling model

As mentioned, the S700MC steel with a high yield point was selected to determine the roll-leveling process parameters, ensuring the sheets' best flatness with an acceptable level of residual stresses. Two roll leveler types were used in the current study, namely 13 and 17 roll versions. Again, the three thicknesses (T) of 3 mm, 5 mm, and 10 mm, which are commercially available for this steel grade, were analyzed. Three-millimeter and 5-mm thick sheets were subjected to leveling simulation using the developed numerical model of the 17-roller machine. The 5 mm and 10 mm sheets were subjected to leveling simulation using the model of the 13-roller machine.

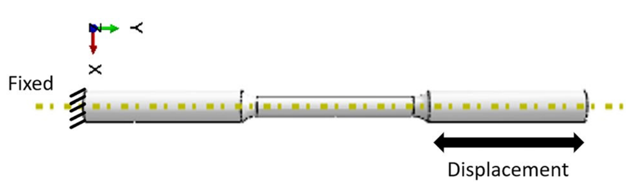

Fig. 5 Finite element model setup of the investigated tension/compression test

During the analysis, various roll diameters (D), distances between subsequent rolls (S) (Fig. 9), rolls vertical arrangements, and plastification ratios (P) during leveling were investigated to evaluate their influence on both the sheet flatness and the level of residual stresses. The vertical roll arrangement of the upper rolls changes linearly from the first to the last roll. The last roll setup (termed "Out" in Tables 3 and 4) is always equal to the plate thickness, while the initial roll setup (termed "In" in Tables 3 and 4) changes according to the required plastification level.

The numerical experiment's plan for the set of analyzed process variants is presented in Tables 3 and 4. In each case, the first and the last roll positions were used to determine the leveler setup, while other rolls were linearly aligned.

a.

The initial flatness was determined based on a series of experimental measurements from the industrial floor realized after the uncoiling stage of the sheet of 2000 mm width (Fig. 10).

Based on these measurements, the initial sheet flatness in the numerical model was assumed at the level of 40 mm at the length of 1000 mm, as seen in Fig. 11.

Three models of sheet steel with a length of 3500 mm and the following thicknesses: 3 mm, 5 mm, and 10 mm were developed to meet the numerical simulation plan (Fig. 12). In each case, the width of the plate in the numerical model was defined as 2000 mm to match the actual width.

In total, the numerical experiment plan comprised 108 numerical FE simulations. The analysis was again performed using a commercial Abaqus FE software and the identified combined hardening model.

The numerical models were also reduced to 2D space to minimize the complexity and computational effort. The models of subsequent rolls were assumed to be rigid during the analysis. Such an approach minimizes the numerical complexity and allows for the assembly of its components, taking into account the contact conditions and disregarding the impact of the density of nodes in the finite element mesh. With such simplification, the computational effort was reduced to the levels acceptable by the industrial requirements; however, it has to be mentioned that the simulation times depend on the sheet thicknesses. Examples of

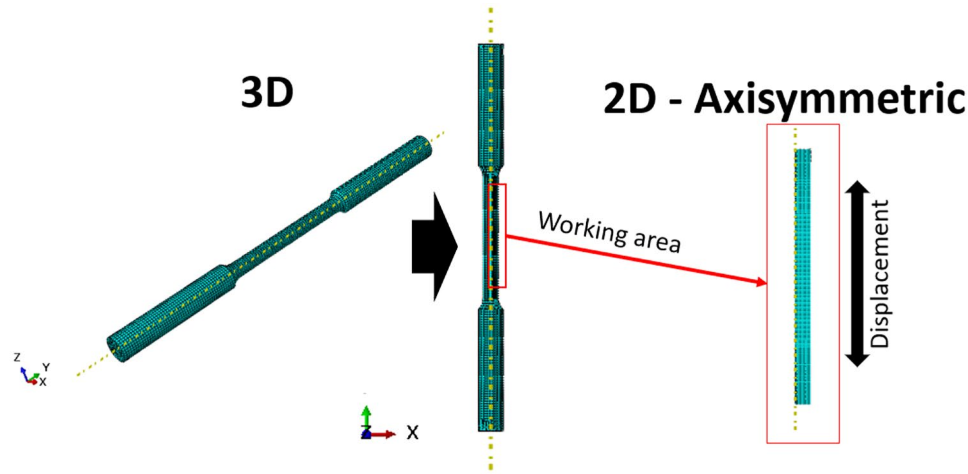

Fig. 6 Finite element model order reduction procedure

developed roll leveler models for the 17 and 13 roller case studies are presented in Fig. 13.

As seen in Fig. 13, an additional straight part of the sheet, 1000 mm in length, was introduced to allow the initial contact between the rolls and the material. This part is only required for the simulation's first step, where the rollers are lowered onto the sheet to reach the defined settings. This section of the steel sheets was not considered during the result analysis stage. The sheet model was discretized by finite elements to obtain a structural mesh. In this case, the elements have the same size and shape. This solution was used after a series of preliminary simulations where anisotropic meshes, also refined in some sheet regions, were used. However, the approach extended the simulation times significantly and could not be used for further investigation. Therefore, the designed mesh is characterized by regularly distributed nodes over the entire cross-section. The global size of the finite element mesh varied for each plate thickness. For the 3 mm sheet, it was 0.6 mm; for 5 mm, it was 1 mm; and for 10 mm, it was 2 mm. The entire set of finite element models for different roll leveler setups was developed with the same assumptions. Finally, the boundary conditions that replicate the leveling setup for upper and lower rolls were defined, as seen in Fig. 14.

In this case (Fig. 14), the roll displacement is fixed along the x and y directions, while the defined velocities ω control their rotation along the z axis. The roll velocities were set to get the linear velocity of $750\frac{\mathrm{mm}}{\mathrm{s}}$, to match the typical conditions used on the industrial floor. The interaction between the sheets and the rolls also considers friction defined by the Coulomb law with the friction coefficient set to 0.25. Prior to the series of finite element analyses, the developed leveling model assumptions were confirmed against the theoretical calculations of the plastification level with four selected case studies, as seen in Fig. 15.

Finally, after the model development and validation stages, a series of simulations were realized to cover the entire plan from Table 2. Examples of the stress and strain field development under subsequent bending operations for the 17 and 13 roll levelers are shown in Figs. 16 and 17, respectively.

The summary of the complete set of 108 numerical simulations from the final flatness point of view is presented in Fig. 18. The flatness of the plates was calculated after the leveling and springback that occurred after the process. The names of the results correspond to the information from Tables 3 and 4.

From Fig. 18, it can be concluded that the best flatness after processing on the 13 roll levelers is obtained for the smallest roll diameter. This behavior is consistent across the wide range of investigated setups. For roll diameters, 130 mm and 140 mm, results are slightly worse and achieve values 6–9 mm, which is close to the acceptable limit of 9 mm. At the same time, the distance between subsequent rolls does not show a significant influence on the flatness of

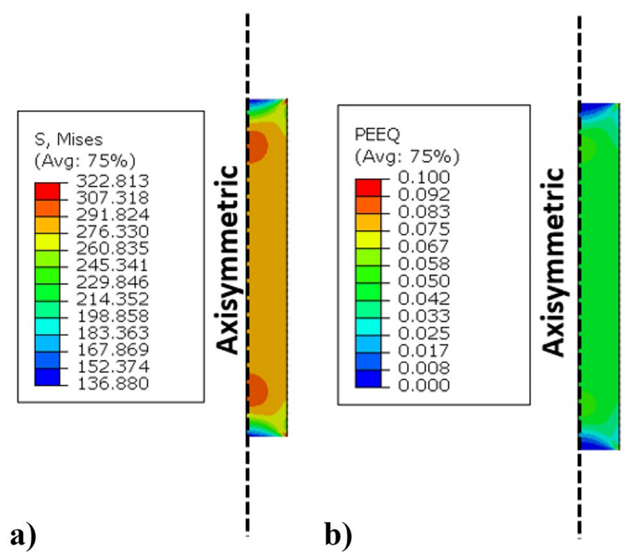

Fig. 7 Equivalent **a** stress, and **b** strain fields obtained at the deformed sample's cross-section after 5 cycles of the tension/compression

Table 2 Identified parameters of the combined hardening model

	σ_0(MPa)	C_1(MPa)	γ_1	Q(MPa)	b
S700MC	550	110,000	250	−60	100

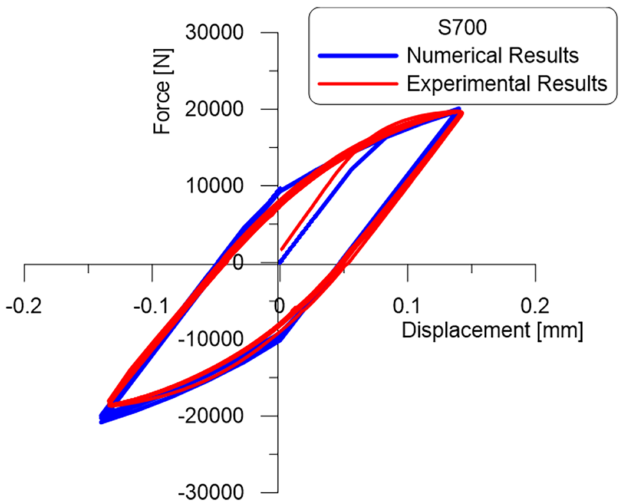

Fig. 8 Comparison of the load–displacement curves calculated and measured during subsequent cycles of the tension/compression

the sheet. On the other hand, for the 17 roll case, obtained flatness results for all the investigated setups are very similar, with differences in flatness at the range of 1 mm. However, as mentioned, appropriate flatness is only one of the criteria used in the current work to evaluate the leveling process capabilities. The other is focused on the level of residual stresses at the surfaces of the sheet. Therefore, stress components in the normal direction were measured along the entire upper and lower sheet surfaces, according to the concept from Fig. 19. This investigation was done for all the simulated case studies, and examples of measurements are illustrated in Fig. 20.

The summary of the results illustrating which of the analyzed systems of leveling machines made it possible to obtain a sheet's satisfactory state, from flatness and stress level point of view, after straightening is summarized in Fig. 21. The information in the upper rows of the table in

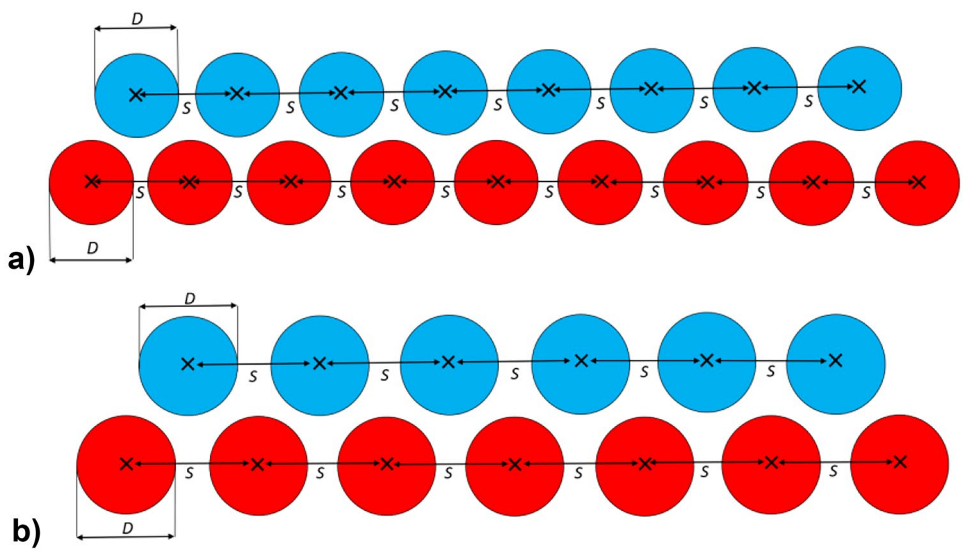

Fig. 9 The investigation roll diameter and roll spacing for the **a** 17 rolls, and **b** 13 roll levelers

Table 3 Numerical experiment plan for various process designs and setups for the 17 rolls

a)

T [mm]	D [mm]	S [mm]	P [%]	In	Out	Name
3	73	78	60	-4.5	3	T3_D73_S78_P60
			70	-6	3	T3_D73_S78_P70
			80	-7.5	3	T3_D73_S78_P80
		79	60	-4.5	3	T3_D73_S79_P60
			70	-6	3	T3_D73_S79_P70
			80	-7.5	3	T3_D73_S79_P80
		80	60	-4.5	3	T3_D73_S80_P60
			70	-6	3	T3_D73_S80_P70
			80	-7.5	2	T3_D73_S80_P80
	76.2	81.5	60	-4.5	3	T3_D76.2_S81.5_P60
			70	-6	3	T3_D76.2_S81.5_P70
			80	-7.5	3	T3_D76.2_S81.5_P80
		82.55	60	-4.5	3	T3_D76.2_S82.55_P60
			70	-6	3	T3_D76.2_S82.55_P70
			80	-7.5	3	T3_D76.2_S82.55_P80
		84	60	-4.5	3	T3_D76.2_S84_P60
			70	-6	3	T3_D76.2_S84_P70
			80	-7.5	3	T3_D76.2_S84_P80
	80	86	60	-4.5	3	T3_D80_S86_P60
			70	-6	3	T3_D80_S86_P70
			80	-7.5	3	T3_D80_S86_P80
		87	60	-4.5	3	T3_D80_S87_P60
			70	-6	3	T3_D80_S87_P70
			80	-7.5	3	T3_D80_S87_P80
		88	60	-4.5	3	T3_D80_S88_P60
			70	-6	3	T3_D80_S88_P70
			80	-7.5	3	T3_D80_S88_P80

b)

T [mm]	D [mm]	S [mm]	P [%]	In	Out	Name
5	73	78	60	0	5	T5_D73_S78_P60
			70	-1.5	5	T5_D73_S78_P70
			80	-3	5	T5_D73_S78_P80
		79	60	0	5	T5_D73_S79_P60
			70	-1.5	5	T5_D73_S79_P70
			80	-3	5	T5_D73_S79_P80
		80	60	0	5	T5_D73_S80_P60
			70	-1.5	5	T5_D73_S80_P70
			80	-3	5	T5_D73_S80_P80
	76.2	81.5	60	0	5	T5_D76.2_S81.5_P60
			70	-1.5	5	T5_D76.2_S81.5_P70
			80	-3	5	T5_D76.2_S81.5_P80
		82.55	60	0	5	T5_D76.2_S82.55_P60
			70	-1.5	5	T5_D76.2_S82.55_P70
			80	-3	5	T5_D76.2_S82.55_P80
		84	60	0	5	T5_D76.2_S84_P60
			70	-1.5	5	T5_D76.2_S84_P70
			80	-3	5	T5_D76.2_S84_P80
	80	86	60	0	5	T5_D80_S86_P60
			70	-1.5	5	T5_D80_S86_P70
			80	-3	5	T5_D80_S86_P80
		87	60	0	5	T5_D80_S87_P60
			70	-1.5	5	T5_D80_S87_P70
			80	-3	5	T5_D80_S87_P80
		88	60	0	5	T5_D80_S88_P60
			70	-1.5	5	T5_D80_S88_P70
			80	-3	5	T5_D80_S88_P80

Table 4 Numerical experiment plan for various process designs and setups for the 13 rolls

a)

T [mm]	D [mm]	S [mm]	P [%]	In	Out	Name
5	127	136	60	0	5	T5_D127_S136_P60
			70	-1.5	5	T5_D127_S136_P70
			80	-3	5	T5_D127_S136_P80
		138	60	0	5	T5_D127_S138_P60
			70	-1.5	5	T5_D127_S138_P70
			80	-3	5	T5_D127_S138_P80
		140	60	0	5	T5_D127_S140_P60
			70	-1.5	5	T5_D127_S140_P70
			80	-3	5	T5_D127_S140_P80
	130	139	60	0	5	T5_D130_S139_P60
			70	-1.5	5	T5_D130_S139_P70
			80	-3	5	T5_D130_S139_P80
		141	60	0	5	T5_D130_S141_P60
			70	-1.5	5	T5_D130_S141_P70
			80	-3	5	T5_D130_S141_P80
		143	60	0	5	T5_D130_S143_P60
			70	-1.5	5	T5_D130_S143_P70
			80	-3	5	T5_D130_S143_P80
	140	149	60	0	5	T5_D140_S149_P60
			70	-1.5	5	T5_D140_S149_P70
			80	-3	5	T5_D140_S149_P80
		152	60	0	5	T5_D140_S152_P60
			70	-1.5	5	T5_D140_S152_P70
			80	-3	5	T5_D140_S152_P80
		154	60	0	5	T5_D140_S154_P60
			70	-1.5	5	T5_D140_S154_P70
			80	-3	5	T5_D140_S154_P80

b)

T [mm]	D [mm]	S [mm]	P [%]	In	Out	Name
10	127	136	60	6	10	T10_D127_S136_P60
			70	4.5	10	T10_D127_S136_P70
			80	3	10	T10_D127_S136_P80
		138	60	6	10	T10_D127_S138_P60
			70	4.5	10	T10_D127_S138_P70
			80	3	10	T10_D127_S138_P80
		140	60	6	10	T10_D127_S140_P60
			70	4.5	10	T10_D127_S140_P70
			80	3	10	T10_D127_S140_P80
	130	139	60	6	10	T10_D130_S139_P60
			70	4.5	10	T10_D130_S139_P70
			80	3	10	T10_D130_S139_P80
		141	60	6	10	T10_D130_S141_P60
			70	4.5	10	T10_D130_S141_P70
			80	3	10	T10_D130_S141_P80
		143	60	6	10	T10_D130_S143_P60
			70	4.5	10	T10_D130_S143_P70
			80	3	10	T10_D130_S143_P80
	140	149	60	6	10	T10_D140_S149_P60
			70	4.5	10	T10_D140_S149_P70
			80	3	10	T10_D140_S149_P80
		152	60	6	10	T10_D140_S152_P60
			70	4.5	10	T10_D140_S152_P70
			80	3	10	T10_D140_S152_P80
		154	60	6	10	T10_D140_S154_P60
			70	4.5	10	T10_D140_S154_P70
			80	3	10	T10_D140_S154_P80

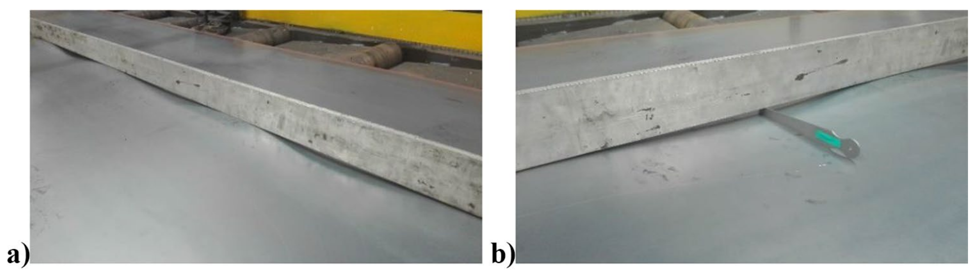

Fig. 10 Initial flatness measurements, **a** general view, **b** enlarged view

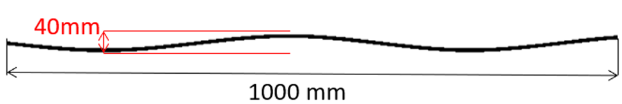

Fig. 11 Initial geometry of the steel sheet prior to the leveling

Fig. 19 corresponds to the leveling setup information from Tables 3 and 4. The last two rows illustrate the numerical simulation results from the flatness and stress point of view. The red color represents simulations results that are not satisfactory. Yellow and green, on the other hand, show

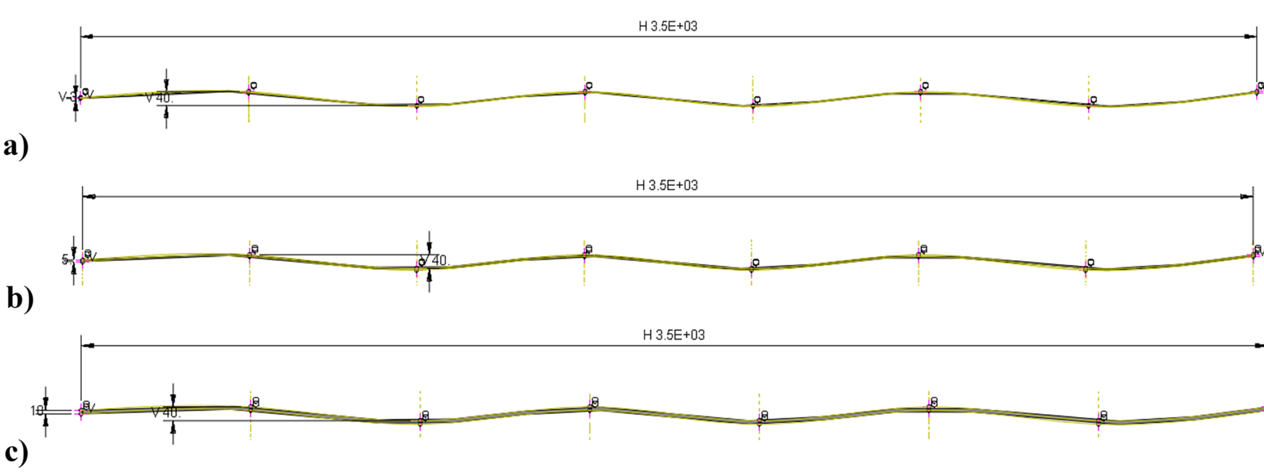

Fig. 12 Sheets geometry for the thickness of **a** 3, **b** 5, and **c** 10 mm

Fig. 13 Examples of the finite element models developed for the **a** 17 and **b** 13 roll levelers

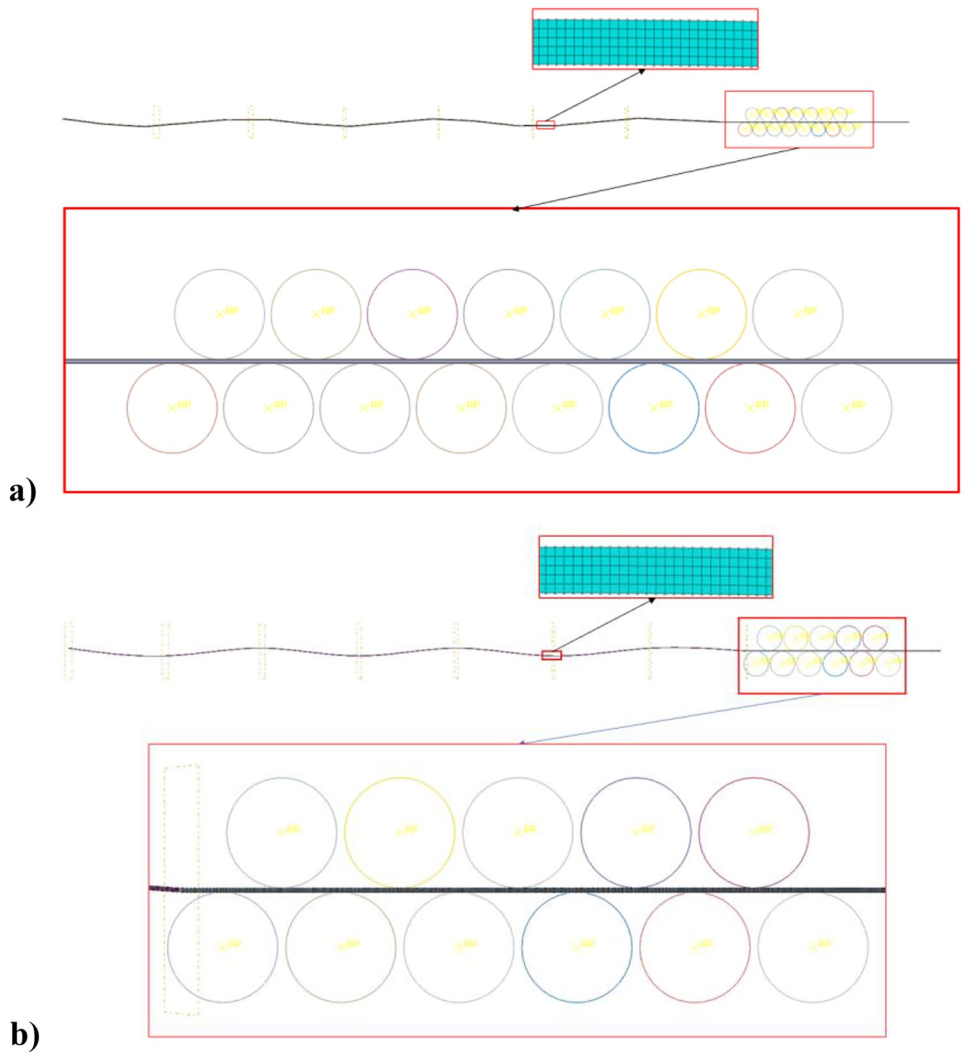

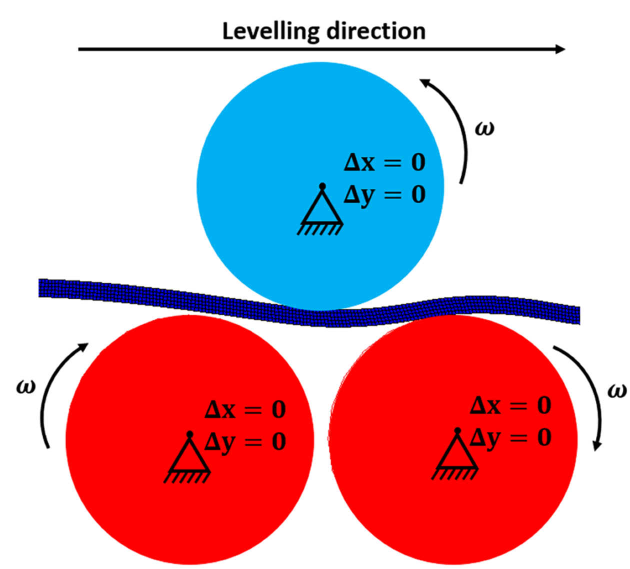

Fig. 14 Boundary conditions applied to upper and bottom rolls

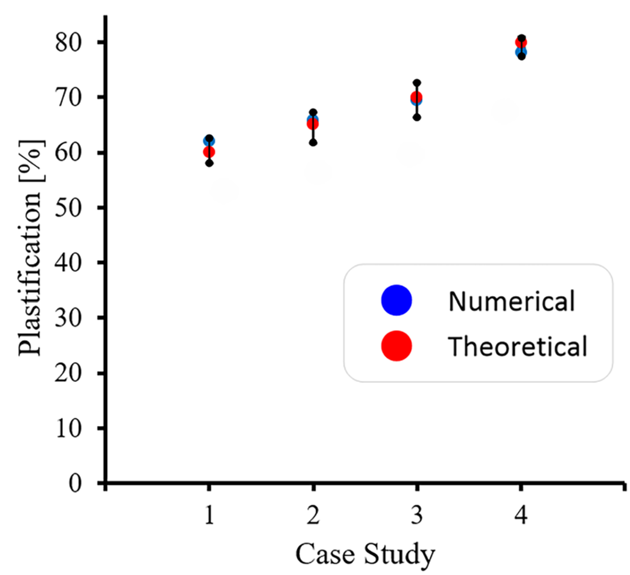

Fig. 15 Comparison of theoretically and numerically predicted plastifications levels

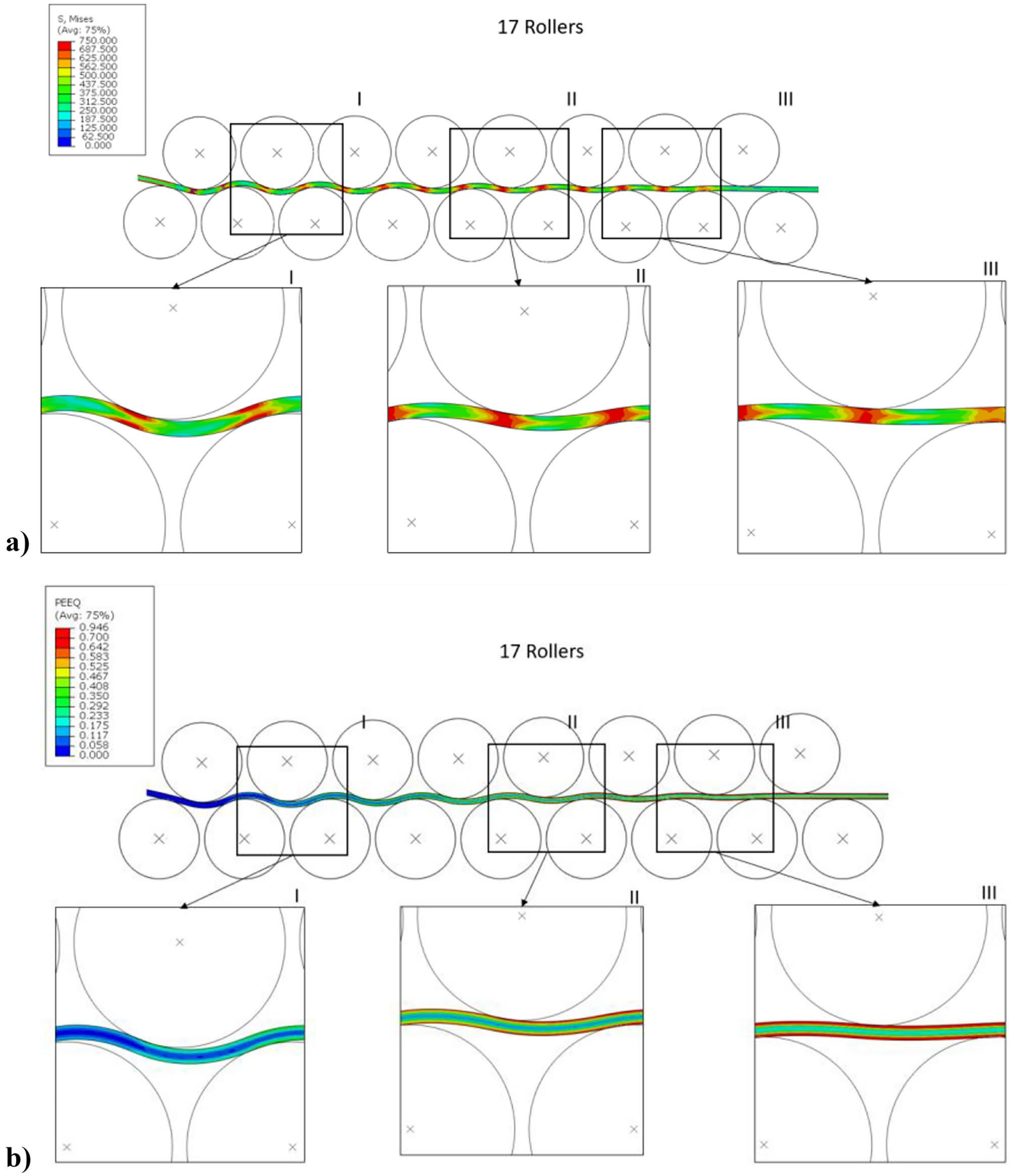

Fig. 16 Example of the **a** stress and **b** strain fields development under subsequent bending operations for the 17 roll levelers and a sheet thickness of 5 mm

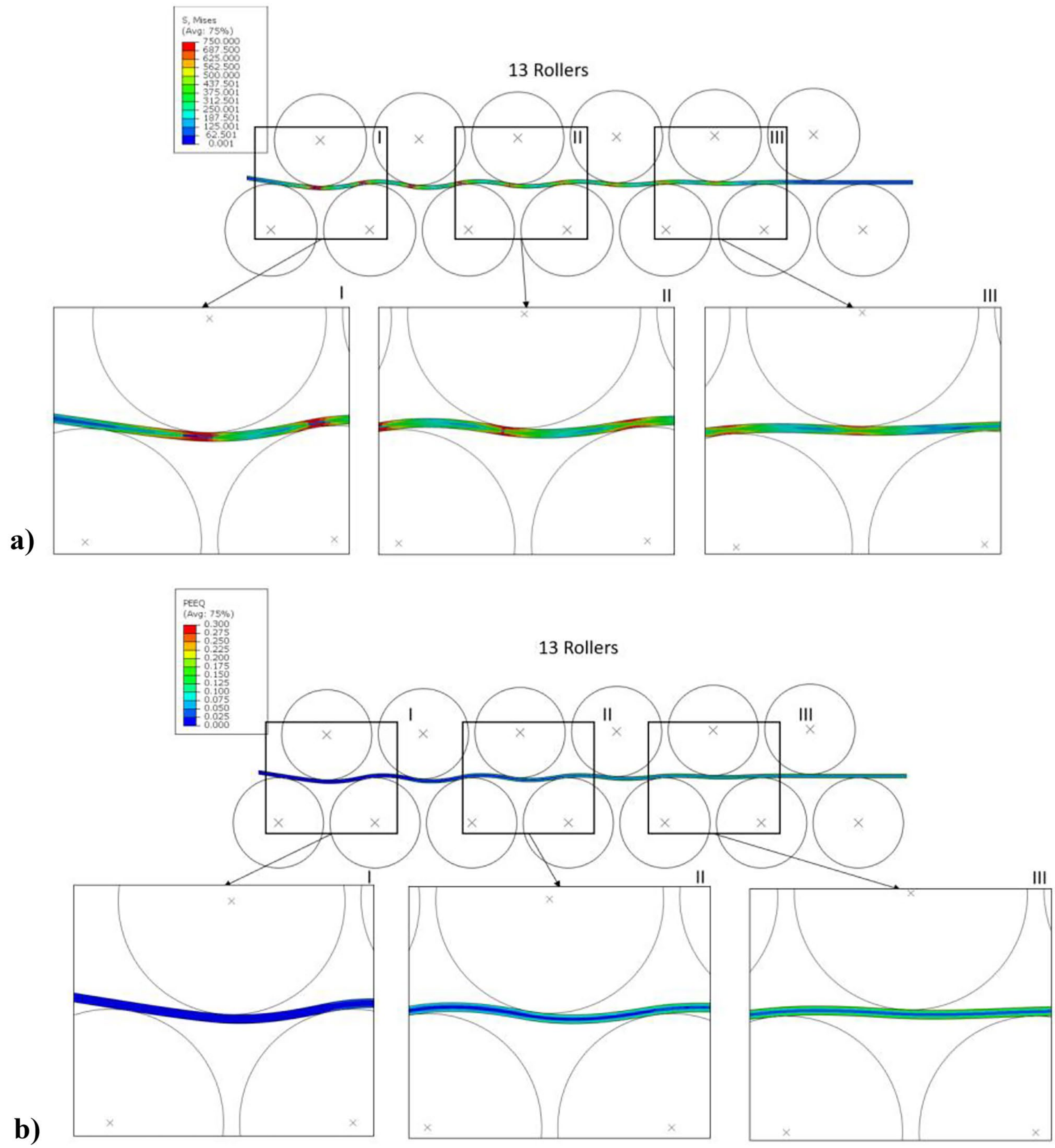

Fig. 17 Example of the **a** stress and **b** strain fields development under subsequent bending operations for the 13 roll levelers and a sheet thickness of 5 mm

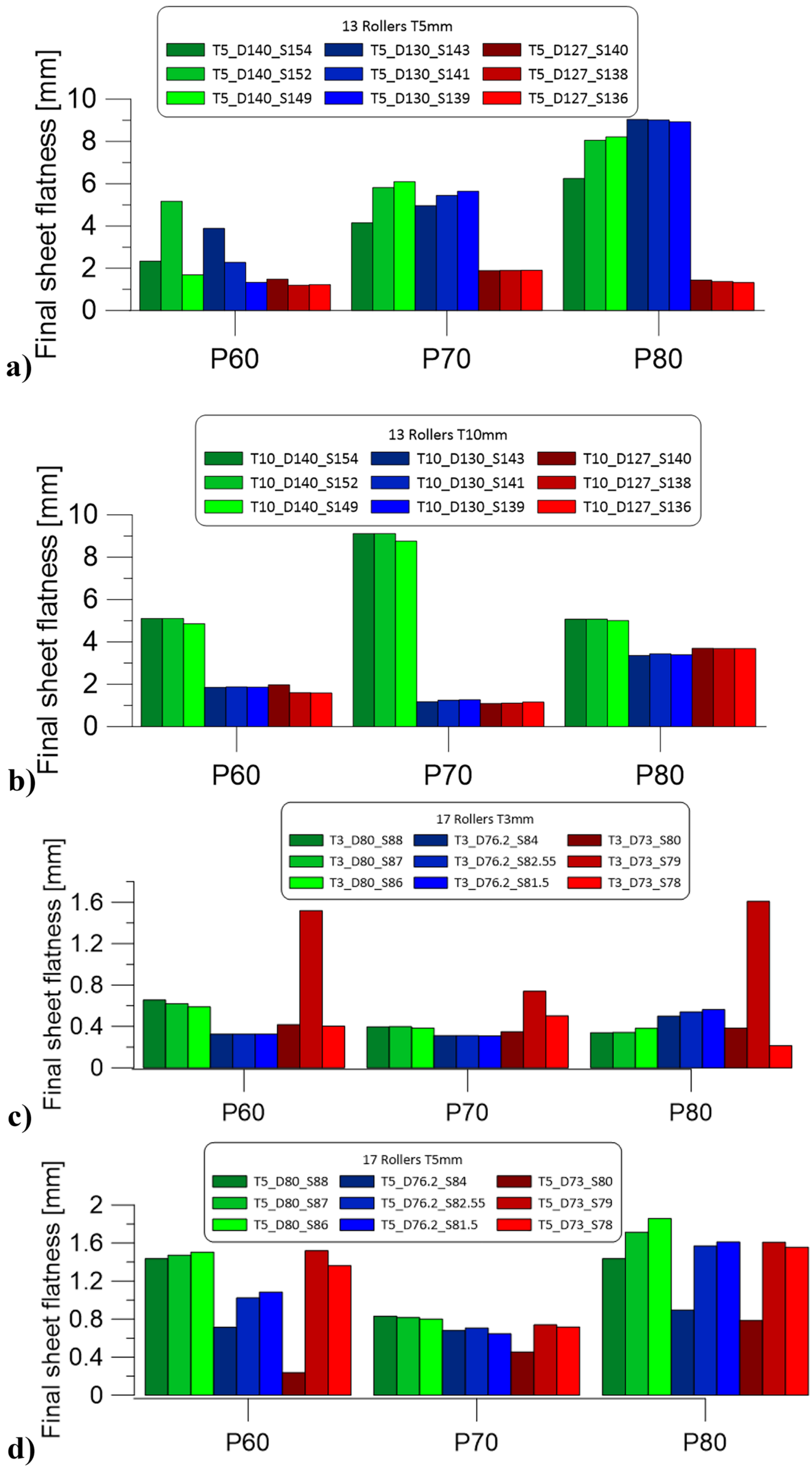

Fig. 18 Final flatness calculated after the leveling for subsequent model setups; **a** 13 roll levelers and 5-mm sheet thickness; **b** 13 roll levelers and 10-mm sheet thickness, **c** 17 roll levelers and 3-mm sheet thickness, **d** 17 roll levelers and 5-mm sheet thickness

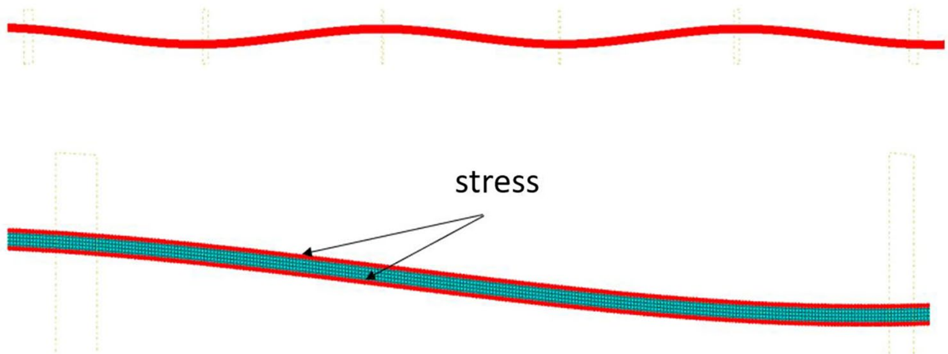

Fig. 19 Measurement setup for stress components in the normal direction after the leveling

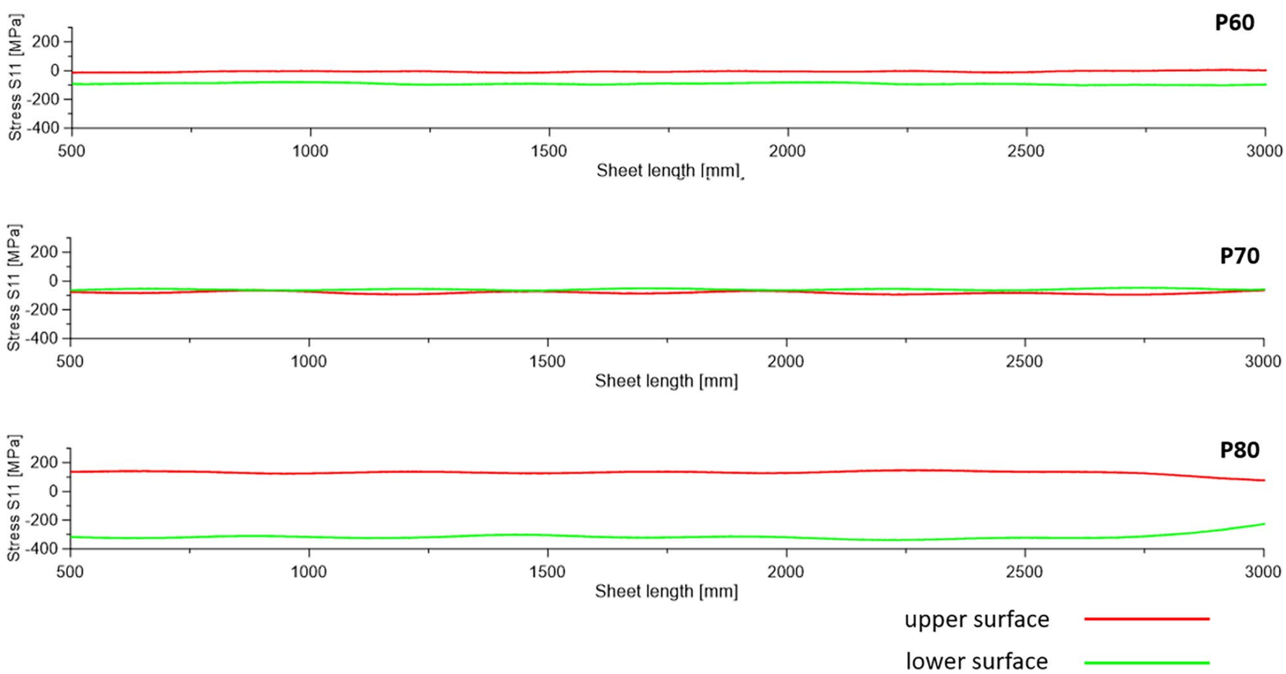

Fig. 20 Stress component in the normal direction calculated on the leveled 10 mm sheet's upper and lower surfaces

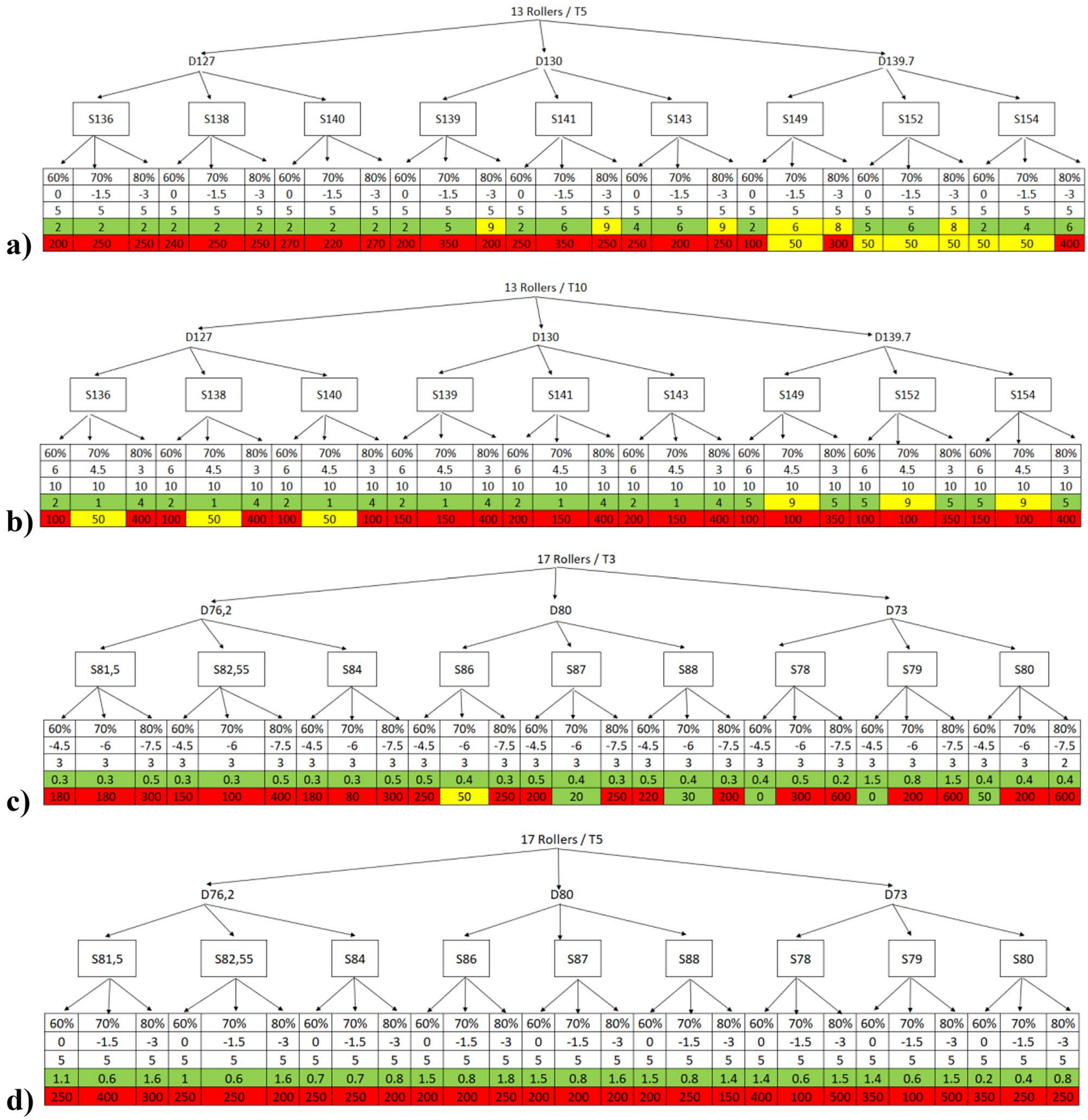

Fig. 21 Summary of the calculated flatness and differences in the stress components for the **a** 13 roll levelers and 5-mm sheet thickness, **b** 13 roll levelers and 10-mm sheet thickness, **c** 17 roll levelers and 3-mm sheet thickness, and **d** 17 roll levelers and 5-mm sheet thickness

simulations results that can deliver a flat product with a reasonable low level of residual stresses that should not affect subsequent processing operations, e.g., laser cutting.

As a result of the analysis, it was determined that flatness should not be the sole criterion for evaluating the quality of the leveled sheet. The stress state plays a major role, and most of the time is in the range that will affect material behavior after the leveling process. At the same time, it can be seen that it is hard to find the optimal geometry of a leveler covering a wide range of thicknesses. A bigger roll diameter of 140 mm allows the achievement of an acceptable stress level for the material thickness of 10 mm, but at the same time, it does not provide good results for the material thickness of 5 mm. In that case, a smaller roll diameter of 127 mm delivers products of better quality. From the entire set of simulations, it was identified that the best parameters for 13 and 17 roll levelers are roll diameter 127 mm with a 140 mm spacing and 70% plastification degree, and a 73-mm roller diameter with a 78 mm spacing and 60%

plastification degree, respectively. Therefore, there are possibilities to obtain a good quality product both from flatness and stress state points of view.

4 Conclusions

The computer-aided technology design was used in this work to evaluate the capabilities of the roll levelers in application to the leveling process of the high-strength steel sheets. A set of leveler setups was selected to match typical industrially available equipment. The reliable hardening model based on the combined isotropic-kinematic approach was developed first using the inverse analysis technique. Then, the extensive numerical simulation plan was executed with the finite element simulation approach. Based on the presented research, the following conclusions can be drawn:

– The state of the leveled steel sheets has to be investigated from a flatness and stress state point of view.
– Leveling operation significantly improves flatness in a wider range of equipment setup; however, the process window from the point of view of the acceptable stress state is much narrower.
– The best-identified parameters for the 13 roll levelers are roll diameter 127 mm with a 140 mm spacing and 70% plastification degree.
– The best-identified parameters for the 17 roll levelers are 73-mm roller diameter with a 78 mm spacing and 60% plastification degree.

The identified leveler setups will also be subjected to further investigation to evaluate their capabilities for the wide range of steel grades and initial flatness levels.

Acknowledgements Financial assistance of the National Center for Research and Development, grant number POIR.01.01.01-00-0786/18 is acknowledged.

Funding Financial assistance of the National Center for Research and Development, grant number POIR.01.01.01–00-0786/18 is acknowledged.

Availability of data and material The raw/processed data required to reproduce these findings cannot be shared at this time as the data forms part of an ongoing study.

Code availability The code for the inverse analysis is an in-house solution.

Declarations

Ethics approval Not applicable.

Competing interests The authors declare no competing interests.

References

1. Wagoner RH, Lim H, Lee M-G (2013) Advanced issues in springback. Int J Plast 45:3–20. https://doi.org/10.1016/j.ijplas.2012.08.006
2. Ulibarri Hernández U, Mendiguren J, Sáenz de Argandoña E, Galdos L, Silvestre E, Gil I (2016) Friction characterisation in levelling processes. Adv Mater Process Technol 2:503–513. https://doi.org/10.1080/2374068X.2016.1247230
3. Smith RP (2007) The effect of the number of leveling rolls on the straightening process. Iron Steel Technol 4:57–68
4. Liu Z, Luo Y, Wang Y, Liao TW (2018) A new curvature analytical method in plate leveling process. ISIJ Int 58:1094–1101. https://doi.org/10.2355/isijinternational.ISIJINT-2017-738
5. Wang Y, Liu Z, Yan X (2012) Evaluation of straightening capacity of plate roll straightener. J Cent South Univ 19:2477–2481. https://doi.org/10.1007/s11771-012-1299-4
6. Silvestre E, Garcia D, Galdos L, de Argandoña ES, Mendiguren J (2016) Roll levelling semi-analytical model for process optimization. J Phys Conf Ser 734:032034. https://doi.org/10.1088/1742-6596/734/3/032034
7. Lee J-B, Kang S-S (2018) Numerical modeling of roller leveler for thick plate leveling. Int J Precis Eng Manuf 19:425–430. https://doi.org/10.1007/s12541-018-0051-x
8. Gavrus A, Massoni E, Chenot JL (1996) An inverse analysis using a finite element model for identification of rheological parameters. J Mater Process Technol 60:447–454. https://doi.org/10.1016/0924-0136(96)02369-2
9. Roucoules C, Pietrzyk M, Hodgson PD (2003) Analysis of work hardening and recrystallization during the hot working of steel using a statistically based internal variable model. Mater Sci Eng A 339:1–9. https://doi.org/10.1016/S0921-5093(02)00120-X
10. Humphreys FJ, Hatherly M (2004) Recrystallization and related annealing phenomena. Elsevier. https://doi.org/10.1016/B978-0-08-044164-1.X5000-2
11. Frederick CO, Armstrong PJ (2007) A mathematical representation of the multiaxial Bauschinger effect. Mater High Temp 24:1–26. https://doi.org/10.1179/096034007X207589
12. Mróz Z (1967) On the description of anisotropic workhardening. J Mech Phys Solids 15:163–175. https://doi.org/10.1016/0022-5096(67)90030-0
13. Chaboche JL, Van KD, Cordier G (1979) Modelization of the strain memory effect on the cyclic hardening of 316 stainless steel. IASMiRT
14. Lemaitre J, Chaboche JL (1990) Mechanics of solid materials. Cambridge University Press. https://doi.org/10.1017/CBO9781139167970
15. Gawad J, Kuziak R, Madej L, Szeliga D, Pietrzyk M (2005) Identification of rheological parameters on the basis of various types of compression and tension tests. Steel Res Int 76:131–137. https://doi.org/10.1002/srin.200505984

16. Madej L, Muszka K, Perzyński K, Majta J, Pietrzyk M (2011) Computer aided development of the levelling technology for flat products. CIRP Ann Manuf Technol 60:291–294. https://doi.org/10.1016/j.cirp.2011.03.137
17. Pietrzyk M, Madej L, Rauch L, Szeliga D (2015) Computational materials engineering. Elsevier. https://doi.org/10.1016/C2013-0-00074-6
18. Szeliga D, Gawad J, Pietrzyk M (2006) Inverse analysis for identification of rheological and friction models in metal forming. Comput Methods Appl Mech Eng 195:6778–6798. https://doi.org/10.1016/j.cma.2005.03.015